

Macroscopic electrostatic potentials and interactions in self-assembled molecular bilayers: the case of Newton black films.

Z. Gamba

Department of Physics - CAC, Comisión Nacional de Energía Atómica,

*Av. Libertador 8250, (1429) Buenos Aires, Argentina. **

(Dated: October 28, 2018)

Abstract

We propose a very simple but 'realistic' model of amphiphilic bilayers, simple enough to be able to include a large number of molecules in the sample, but nevertheless detailed enough to include molecular charge distributions, flexible amphiphilic molecules and a reliable model of water. All these parameters are essential in a nanoscopic scale study of intermolecular and long range electrostatic interactions. We also propose a novel, simple and more accurate macroscopic electrostatic field for model bilayers. This model goes beyond the total dipole moment of the sample, which on a time average is zero for this type of symmetrical samples, i. e., it includes higher order moments of this macroscopic electric field. We show that by representing it with a superposition of gaussians it can be *analytically* integrated, and therefore its calculation is easily implemented in a MD simulation (even in simulations of non-symmetrical bi- or multi-layers). In this paper we test our model by molecular dynamics simulations of Newton black films.

*Electronic address: gamba@tandar.cnea.gov.ar. URL: <http://www.tandar.cnea.gov.ar/~gamba>

I. INTRODUCTION

The structure and dynamics of amphiphilic bilayers plays a key role in numerous problems of interest in physical-chemistry [1], biology [2], pharmacology [3] and biotechnology [4, 5]. Amphiphilic molecules consist of a non-polar hydrophobic flexible chain of the $(CH_2)_n$ type, the 'tail', plus a hydrophilic section, a strongly polar 'head' group. In aqueous solutions the polar 'head' strongly interacts with water and shields the hydrophobic tails from the water, therefore these molecules tend to nucleate in micelles or bilayers, depending on concentration [1]. For example, a simple model of a biological membrane consists of a bilayer of amphiphilic molecules, with their polar heads oriented to the outside of the bilayer and strongly interacting with the surrounding water. The opposite model of bilayer, with the water in the middle and head groups pointing to the inside, also exists in nature and are the soap bubbles films, or Newton black (NB) films, as they are called in their thinnest states. Most studies have been performed on biological membrane models and huge advances in the intermolecular potential models (at atomistic or coarse grained level) needed for their numerical simulations as well as in the behavior of proteins, anesthetics molecules, pores, etc., inserted in these bilayers have been achieved.

Here we will limit our study to the case of soap bubbles films. While on one hand the molecular interactions and macroscopic electrostatic field exhibit the same physical problems to solve as that of the biological membranes, on the other hand the amount of water is limited by the width of the NB film and therefore the numerical simulations are considerable less expensive.

Furthermore, the study of foam films is not only interesting *per se*, but also has many technological applications, in particular their use in biotechnological applications is a very active field. For example, a protein can be unfolded when inserted in these films, allowing a small angle X ray measurement of its structure. In refs. [6, 7] the structure of the film is studied as a function of the concentration of inserted proteins; these measurements give information on the protein-lipids interactions, in much simpler experimental arrays than biological membranes. At the mesoscopic scale, the diffusion of bacteria in this quasi-two-dimensional liquid environment has been measured [8].

From the point of view of applied physics there is also increasing interest in the growth of inorganic nano-patterned films with the help of organic bilayers [9].

Furthermore, recent studies have revived the interest in the basic physics involved in these films. The self-assembly of amphiphilics can be experimentally measured by studying the properties of soap films, with the advantage of a fine control in the range of low contents and small concentration changes of amphiphilics [10]. Also confined water is known to have a very different behaviour of bulk water, its behavior at cryogenic temperatures and its glass transition temperature were measured by anelastic spectroscopy [11] in a stack of biological membranes, but not yet in foam films. In ref. [12] the stability of soap films under different applied capillary pressures has been measured, and in ref. [13] a mean field theory is developed to describe the rôle of electrostatic fluctuations in their stability.

Several MD simulations of NB films have been performed since some time ago. In Ref. [14] a series of all-atom MD simulations of NB films of sodium-dodecyl-sulfate SDS $[\text{Na}^+\text{CH}_3(\text{CH}_2)_{11}(\text{OSO}_3)^-]$ amphiphilic molecules and different amounts of water was presented, and an insight of the experimental electron density profile given by X-ray measurements was obtained [15]. In Ref. [16] these simulations were extended to larger samples and longer times (about nanosec.), a fact that is important to accurately measure the diffusion constants of the lipids in bilayers, even when similar structural and internal dynamical properties can be obtained at shorter times [17]. The effect of several surfactants on the disjoining pressure [18] and the anomalous behavior of water [19] were also investigated *via* MD simulations. The last reference clearly pointed out that the study of electrostatic forces between charged interfaces in aqueous media is still an open and very important field of theoretical research.

Here we are interested in the search of a very simple but 'realistic' model of the Newton black films, simple enough to be able to include a large number of molecules in the sample, but nevertheless detailed enough to include molecular charge distributions, flexible amphiphilic molecules and a reliable model of water. All these parameters are essential in a nanoscopic scale study of intermolecular and long range electrostatic interactions. Such simple amphiphilic bilayer model will be useful to obtain reliable information on the effect of the "external parameters" (like surface tension, external pressure and temperature and

external fields) on physical properties of the bilayer, as well as to address problems like the diffusion and/or nucleation of guest molecules of technological, pharmaceutical or ambiental relevance within amphiphilic bilayers.

A problem to solve in the simulation of these highly charged bilayers is the method to use in the calculation of electrostatic interactions, due to their long range and quasi-bidimensional 2D nature. The Ewald method is assumed to be the accurate one for electrostatic interactions [20] in three dimensional 3D samples. Refs. [21–23] review the 3D Ewald sums as well as several possible implementations, in those papers 3D periodic boundary conditions are used to minimize surface effects and all interacting molecules are explicitly included. However, for single monolayers or bilayers the periodic boundary conditions should be applied in two directions, in the plane of the mono- or bilayers ($x y$ plane), but not along the perpendicular to the plane (z axis). 2D Ewald sums have been developed for these cases, although they are computationally very lengthy by comparison with the 3D sums [24, 25]. Recently Bródka and Grzybowski [26] showed analytically in which way the 2D Ewald sums may be accurately approximated by a 3D calculation. They show that, in order to obtain a reliable calculation, not only a large empty space must be introduced in the simulation box (along z), but the macroscopic electric field term depending on the total dipole moment \mathbf{M} of the sample ($|\mathbf{M}|^2/3$) should be replaced by a term containing only the component z perpendicular to the 2D system (M_z^2). In ref. [27] this result was checked with a numerical simulation. It has to be taken into account that, in a MD simulation, the contribution of this macroscopic electric field to the molecular interactions fluctuates in time and is far from negligible [27], particularly for monolayers.

The core of the paper is in Section IV where we propose a novel, simple and more accurate macroscopic field for model bilayers. That is, a model that goes beyond the total dipole moment of the sample, which on time average is zero for this type of symmetrical bilayers. Following this approach, we extend it by including higher order moments of this macroscopic electric field. We show that by representing it with a superposition of gaussians it can be *analytically* integrated, and therefore its calculation easily implemented in a MD simulation (even in simulations of non-symmetrical bilayers).

In this paper we study a simple model of Newton black films via MD simulations and using the TIP5P intermolecular potential for water and a flexible charged chain to simulate the amphiphilic molecules. We show that our method of calculation of the macroscopic electrostatic potential reproduces the spatial and temporal charge inhomogeneities of the quasibidimensional sample and is extremely simple to implement in numerical simulations. We also show that this method can be directly applied to any other type of bi- or multi-layers.

II. THE AMPHIPHILIC AND WATER MOLECULE MODELS

Our simple model of a charged amphiphilic consists in a semiflexible single chain of 14 atoms, the bond lengths are considered constant, but bending and torsional potentials are included. The first two atoms of the chain mimic a charged and polar head (atom 1 with $q_1 = -2e$, atom 2 with $q_2 = 1e$), sites 3 to 14 form the hydrophobic tail with uncharged atoms: sites 3 to 13 are uncharged united atom sites CH_2 and site 14 is the uncharged united atom site CH_3 . This molecular model correspond to an oversimplification of sodium dodecyl sulfate SDS ($CH_3(CH_2)_{11}OSO_3^- Na^+$) in solution, so we are including, in our simulations, a Na^+ ion per chain. The LJ parameters of these interaction sites are those of ref. [14], except for the sites 1 and 2 that form the amphiphilic polar head: $\sigma_1 = 4.0\text{\AA}$, $\sigma_2 = 4.0\text{\AA}$, $\sigma_{Na} = 1.897\text{\AA}$, $\epsilon_1 = 2.20\text{ kJ/mol}$, $\epsilon_2 = 1.80\text{ kJ/mol}$ and $\epsilon_{Na} = 6.721\text{ kJ/mol}$. The masses of the sites are the corresponding atomic masses, except that $m_1 = m_2 = 48\text{au.}$, in order to mimic the 'real' amphiphilic head. The LJ parameters of the united atom sites are taken from calculations on n -alkanes [28]: $\sigma_{CH_2} = 3.850\text{\AA}$, $\sigma_{CH_3} = 3.850\text{\AA}$, $\epsilon_{CH_2} = 0.664\text{ kJ/mol}$, $\epsilon_{CH_3} = 0.997\text{ kJ/mol}$. The LJ parameters for the Na^+ ion are taken from simulations of SDS in aqueous solution [29] and NB films [14].

The intramolecular potential includes harmonic wells for the bending angles β and the usual triple well for the torsional angles τ , the constants are those commonly used for the united atom site CH_2 [20]. These potentials are needed to maintain the amphiphilic stiffness and avoid molecular collapse. The bending potential is

$$V(\beta) = k_{CCC}(\beta - \beta_0)^2 ,$$

with $\beta_0 = 109.5\text{ deg.}$ and $k_{CCC} = 520\text{ kJ/rad}^2$. The torsional potential is of the form

$$V(\tau) = a_0 + a_1 \cos(\tau) + a_2 \cos^2(\tau) + a_3 \cos^3(\tau) + a_4 \cos^4(\tau) + a_5 \cos^5(\tau) ,$$

the constants are $a_0 = 9.2789$, $a_1 = 12.1557$, $a_2 = -13.1202$, $a_3 = -3.0597$, $a_4 = 26.2403$ and $a_5 = -31.4950 \text{ kJ/mol}$; this potential has a main minimum at $\tau = 0 \text{ deg.}$ and two secondary minima at $\tau = \pm 120 \text{ deg.}$

The selected molecular model for water is the classical rigid molecular model TIP5P [30, 31]. It consists of one LJ site ($\varepsilon = 0.67 \text{ kJ/mol}$, $\sigma = 3.12 \text{ \AA}$) localized at the O and 4 charges. Two charges $q_{\text{H}} = 0.241e$ are localized at the H atoms and two $q_{\text{LP}} = -q_{\text{H}}$ at the lone pairs. As the lone pair interaction sites are not coincident with atomic sites, the algorithm employed to translate the forces from massless to massive sites is that of ref. [32]. The final version of the MD program is similar to that used in refs. [33–35].

This rigid, nonpolarizable, TIP5P molecular model was selected by us because it is simple and it also gives good results for the calculated energies, diffusion coefficient and density ρ as a function of temperature, including the anomaly of the density near 4C and 1atm [30], the X-ray scattering of liquid water [36], etc. The only exception is the O-O pair correlation function $g_2(r)$, for which the first neighbor is located at a slightly shorter distance than the experimental one [30]. Very recently a six sites rigid model for water [37], with an additional site at the molecular center of mass, has been presented. By comparison with the TIP5P model, the new model has improved the fit of the melting point and the disordered structure of ice at the melting point. Nevertheless, this six sites model still shows the same problem of TIP5P to reproduce the experimental $g_{\text{OO}}(r)$ pair correlation function and this is the reason to perform our calculations with TIP5P.

III. THE MODEL BILAYER OF AMPHIPHILIC MOLECULES:

Fig. 1 shows the initial configuration of one of our simple model of a NB film (i. e. soap bubbles films) with the water within the bilayer and, therefore, the head groups oriented to the inside. The sample of the figure includes 226 amphiphilics and 365 water molecules, and, as in model (a), the bilayer is perpendicular to the \hat{z} MD box axis, with a box size of $a = b = 45. \text{ \AA}$, $c = 1000 \text{ \AA}$.

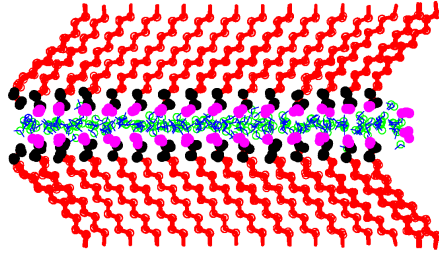


Figure 1: Initial configurations of a model Newton black film.

The periodic boundary conditions are applied only in the \hat{x} and \hat{y} direction and a large unit cell c parameter (that is, a large empty volume) is taken, in order to approximate the required 2D Ewald sums by the usual 3D sums plus our macroscopic field term corresponding to a quasi-2D system, discussed in the following section.

When performing these simulations, we have to take into account, in particular, the following facts:

a) The site-site LJ interactions between all molecules in the sample have a finite cut-off radius of 15 \AA . In 3D simulations, the contributions of sites outside this sphere are taken into account assuming an uniform distribution of sites and performing a simple integration. In our cuasi 2D system, the volume to integrate is that outside the cut-off sphere and within the volume of the slab. Appendix A includes this integral.

b) The electrostatic interactions are calculated *via* the standard 3D Ewald sums with a large size box along the perpendicular to the bilayer slab and 2D periodic boundary conditions in the plane of the slab. The Ewald's sum term corresponding to the macroscopic electric field is discussed in the following section.

IV. THE MACROSCOPIC ELECTRIC FIELD IN A QUASI - 2 D SAMPLE:

Electrostatic forces have a far from negligible contribution to the self-assembly and final patterns found in soft matter systems. For bilayers the macroscopic electric field is given, in a first approximation, by the contribution of the surface charges of the macroscopic dielectric

slab. There are very clear reviews where the first multipolar moment of these charges are taken into account, in 2D and 3D macroscopic samples [25, 27]. In particular, for an uniform dielectric slab oriented perpendicular to the z direction, the contribution of the uniformly distributed surface charges to the total energy of the macroscopic slab system, of volume V , is:

$$U^{macrosc.} = \frac{2\pi}{V} M_z^2,$$

where M_z is the total dipole moment of the slab. Then the contribution of this term to the total force on every charge q_i of the sample is:

$$F_i^{macrosc.}(z) = -\frac{4\pi}{V} M_z.$$

This approximation has been tested in monolayers [26, 27]. In the MD simulation of bilayers, and due to its geometry, the total dipole moment M_z is zero in a time average. Nevertheless, as in monolayers the forces $F_i^{macrosc.}(z)$ are not negligible by comparison with the rest of the interaction forces, and, as the electrostatic interactions play a key rôle in the dynamics and structural properties of the bilayers, a more accurate estimation of their macroscopic electric field is desirable. One possibility is to include higher multipolar moments of the surface charges, but the convergence of the electrostatic interactions using total multipole series is slow. Another possibility is to solve the Poisson-Boltzman equation with boundary conditions given by the surface charges [38], this method is extremely lengthy for a numerical simulation, because the charged atoms are mobile and change their location in every time step.

Nagle & Nagle [39, 40] recently reviewed the experimental data on the structure of lipid bilayers, in particular the distribution functions for the symmetrical components along the direction of the normal to the bilayer. They analyze not only the peak positions of each distribution but their shape, pointing out that they are slightly asymmetrical (to the interior or exterior of the bilayer) and therefore a gaussian distribution model is just an useful first approximation when only the positions and widths are available.

Here we propose a novel coarsed fit for the charge distribution of the different bilayer components (water and charged amphiphilics plus ions) using a superposition of gaussian distributions. We found that, in this way, the contribution of these charge distributions to the macroscopic electric field can be exactly calculated. The method is extremely simple to

implement in numerical simulations, and the spatial and temporal charge inhomogeneities are roughly taken into account. Our results can also be applied to biological membrane models.

At each time step of the MD simulation we decompose our bilayer's charge distribution in four neutral slabs: two for the upper and lower water layers and other two for the neutral layers formed by the head plus ion charges.

For each one of the four neutral slabs, instead of consider two planar surfaces with an uniform density of opposite charges, we propose two gaussian distribution along z , the perpendicular to the slabs, with the same opposite total charges and located the same relative distance (maintaining the slab width). The coarsed distribution of charges in the bilayer is then a linear superposition of gaussians:

$$\rho(z) = \sum_i \frac{q_i}{\sqrt{2\pi}\sigma_i} \exp\left(-\frac{(z-z_i)^2}{2\sigma_i^2}\right) \quad ,$$

The macroscopic electric potential $V(z)$ and the force field $E_z(z)$ due to this type of charge distribution can be exactly solved. In Appendix B we include the analytically solved integrals (one of them is a new mathematical solution). The final result is:

$$\begin{aligned} V(z) &= -2\sqrt{2\pi} \sum_i \sigma_i q_i \left(\exp\left(-\frac{(z-z_i)^2}{2\sigma_i^2}\right) - \left(\frac{z-z_i}{\sqrt{2}\sigma_i}\right) \text{Erf}\left[\frac{(z-z_i)}{\sqrt{2}\sigma_i}\right] \right). \\ E_z(z) &= -\frac{\partial V(z)}{\partial z} = 2\pi \sum_i q_i \text{Erf}\left[\frac{(z-z_i)}{\sqrt{2}\sigma_i}\right]. \end{aligned}$$

The obtained result is valid for any number of slabs, that as a function of time can change not only their position and width but also they can superpose. The practical implementation of this macroscopic field in our simulations (that is, how the σ_i , z_i and q_i values are taken at each time step) is explained in the following section.

The contributions of this macroscopic field, as well as that of the external field $U_{eff}(h)$ in biological membranes, calculated for several bilayers samples are included in section 7. Units: density of charges $[\rho] = \frac{e}{\text{\AA}^3}$; electrostatic potential $[V] = \frac{e}{\text{\AA}}$ (for comparisson with experimental data $\left[\frac{e}{\text{\AA}}\right] = 0.04803 \frac{cm^{1/2}gr^{1/2}}{sec} = 14.399 [Volt]$); electric field $[E] = \frac{e}{\text{\AA}^2}$.

Here we have applied this exact calculation method of the macroscopic electric field to a symmetrical (along z) slab geometry, but it is also valid in an asymmetrical case, which

may imply a finite difference of potential across the bilayer.

The extension of this method (a coarse grained representation of the macroscopic electric field *via* a superposition of gaussians) to other geometries is also strightforward, a spherical geometry, for example, would be useful for the study of miscelles. Its great advantage is that these representations can be *analytically* solved. Moreover, although the present work is not dedicated to the study of reaction fields, based on a coarse gaussian distribution of charges, can be also be easily applied to include a more realistic reaction field inside a cavity in non-uniform dielectrics.

V. IMPLIMENTATION OF THE NUMERICAL SIMULATIONS:

In our MD simulations of the bilayers of Fig. 1, the integration algorithms, time step and cut-off radius are essentially identical to those used on our bulk samples [33, 35], except for the periodic boundary conditions, that now are applied only in the xy plane of the bilayers, and that the calculations include now our proposed macroscopic electric field. The equations of motion of the rigid water molecules are integrated using the velocity Verlet algorithm for the atomic displacements and the Shake and Rattle algorithms for the constant bond length constraints on each molecule. The time step is of 1 fs., the sample is thermalized for 20 ps. and measured in the followings 100 ps.

To maintain a constant temperature in our simulations of these bilayers, the Nosé-Hoover chains method [41] (that we previously used for bulk samples) was disregarded because of the lenthly termalization of all the components, in many cases we obtained a different equilibrium temperature for each different molecular species. Instead, we chose to perform our MD simulations of the bilayers using the Berendsen algorithm [42], applying the equipartition theorem to each type of molecule and a strong coupling constant $\tau = 0.5 \Delta t$ linking the average kinetic energy of each kind of molecules (amphiphilics, ions and water) to the desired kinetic energy of $\frac{3}{2}k_B T_0$, with $T_0 = 300K$. The Berendsen algorithm attains equipartition and equilibrium temperatures faster than the Nose-Hoover chains method, when applied to our mix of flexible and rigid molecules.

To include the macroscopic electric field term we need to determine the values of the σ_i ,

z_i and q_i parameters at each MD time step. For each one of the two slabs that simulate the charge distribution of chains' heads plus ions, we fit the z_i parameters of two gaussians, so as to reproduce the dipolar moment of the slab. Their σ_i values are obtained from the corresponding charge distributions, with $q_i = 1$ for ions and $q_i = -1$ for chains' heads. Typical values of these variables, as well as the contribution of the external potential and the macroscopic electric field to the total forces on all molecules, are reported for each calculated case.

VI. RESULTS:

Here we present the results obtained for one sample of our simple NB film model. Our simulations were mainly performed to analyze the contribution of the macroscopic electric fields to the equilibrium structure and molecular dynamics of the bilayer. Elsewhere we will test the versatility of our approach by studying biological membrane models with and without ions solved in water, with and without the water layer, as a function of chain length, etc..

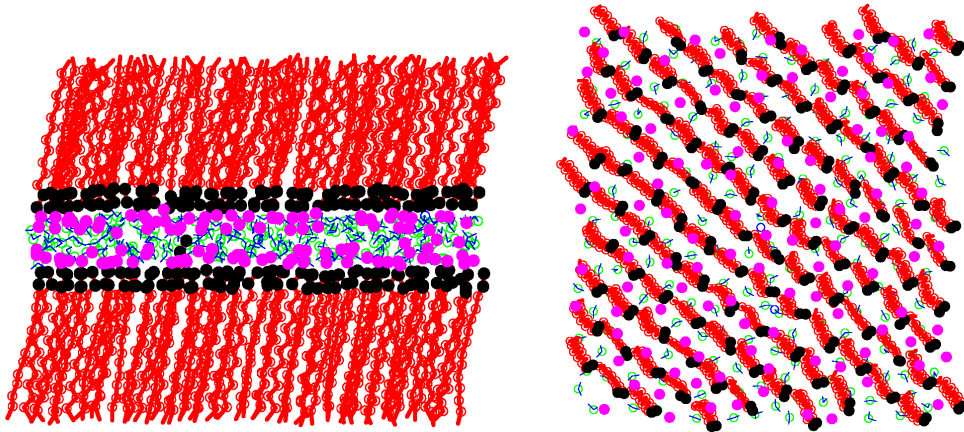


Figure 2: Final configuration of the HD sample with $a=b=45\text{\AA}$: (a) ac cross section, (b) ab cross section.

In Ref. [14] a MD simulation with 64 all-atom sodium-dodecyl-sulfate SDS $[\text{Na}^+\text{CH}_3(\text{CH}_2)_{11}(\text{OSO}_3)^-]$ molecules and 1 to 6 water molecules per amphiphilic was presented. Here we use our simplified amphiphilic model. In section 4, Fig. 1 (b) showed the initial configuration of a sample consisting of 226 charged amphiphilics and

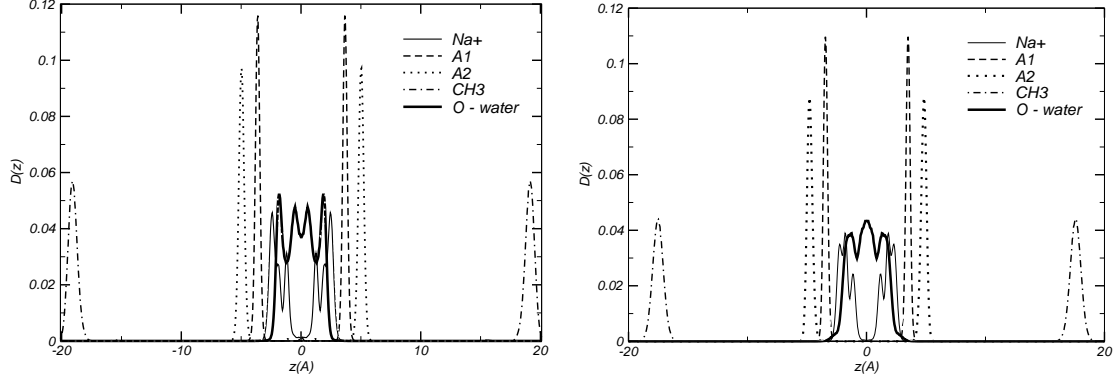


Figure 3: Atomic density profiles (number of atoms per \AA^3) for the (a) HD and (b) LD head group samples.

226 Na^+ ions solved in 365 water molecules, the bilayer is perpendicular to the \hat{z} MD box axis, with a box size of $a = b = 45.5\text{\AA}$, $c = 1000\text{\AA}$. The film is thermalized for 50 ps. and measured in the following 100 ps., Fig. 2 shows the attained final configuration of this sample (HD high density), two other samples with a lower density of amphiphilic heads per unit area were calculated: a medium density MD ($a = b = 46.5\text{\AA}$) and a LD low density sample ($a = b = 48.0\text{\AA}$).

The width of our HD film is 38.2\AA , of our MD film is 36.8\AA and that of the LD one is 35.1\AA , as measured from the average distance between end tail CH_3 groups. Fig. 3 shows the atomic density profiles in two cases. X-ray reflectivity measurements determined that common soap films (CBF) are several thousand angstroms wide, while a NBF is about 33\AA [15]. In ref. [43] a dual optical multiwave interferometer (of $\lambda = 1.064\mu m$) was used to determine the dynamics of gravity induced gradients in soap film thicknesses, which allows to detect variations of about 1\AA in the thickness of the film.

The three cases correspond to a glassy phase, as measured by their diffusion coefficients. For the HD sample the molecular centers of mass location show average oscillations with an amplitude of $\sim 3\text{\AA}$ and we measured an overall displacement of about 5\AA in 100 ps., within the bilayer plane, therefore our measured diffusion coefficient is less than our measurement error (about $10^{-6}cm^2/sec$). The experimental value of the diffusion coefficient for SDS, in a film of about 35\AA thickness, is $6 \cdot 10^{-7}cm^2/sec$ [7, 44] . In the MD and LD samples

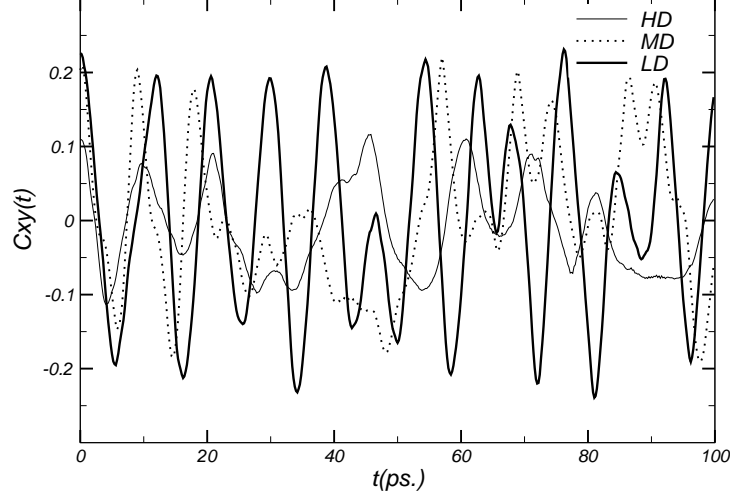


Figure 4: Reorientational autocorrelation in the xy plane.

we observe a collective rotation or large amplitude oscillation of the amphiphilic molecules around their corresponding center of mass and about an axis perpendicular to the bilayer plane. We measure a tilt angle of 26.2 deg. in our HD sample, 35.9 deg. in the MD and 40.2 deg. in the LD sample. Fig. 4 shows the autocorrelation function of the xy component of the reorientational molecular motion, showing a disordered reorientation at HD and an oscillatory motion at LD.

As in the previous bilayers models, the function $\rho(z)$ is obtained from a coarse grained fit of the charge distribution of our MD sample using four charged slabs. The parameters that describe these slabs are for the LD film are:

	$q_i(e)$	$z_i(\text{\AA})$	$\sigma_i(\text{\AA})$	
<i>slab 1 (head and ions)</i>	-1.0	3.485	3.344	
	1.0	2.733	3.344	
<i>slab 2 (water)</i>	-0.241	1.196	0.433	
	0.241	3.762	0.433	,
<i>slab 3 (water)</i>	0.241	-3.762	0.433	
	-0.241	-1.196	0.433	
<i>slab 4 (head and ions)</i>	1.0	-2.733	3.344	
	-1.0	-3.485	3.344	

and with them we calculate the functions included in Fig. 5 (a) . As this is a very thin NB film with about 1.6 water molecules per amphiphilic, water is highly packed and strongly

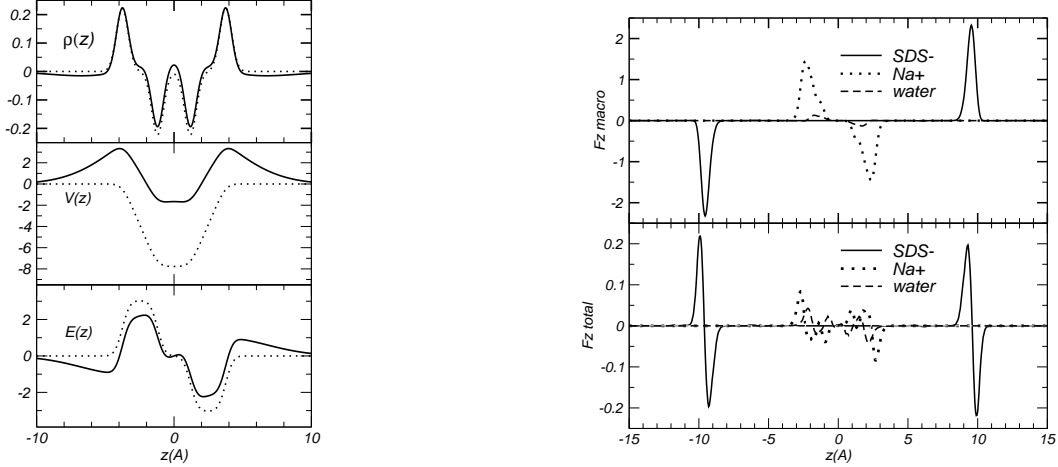


Figure 5: Profile of: (a) the macroscopic charge density $\rho(z)$, electric field and potential (full line for total values, dotted line for water contribution), (b) our measured profile of macroscopic electric and total forces on molecules, as a function of the location of their centers of mass along z , in the HD, NB film.

polarized due to the electric field generated by the charged head and ions. In Fig. 5 (a) we also included the strong contribution of the water layer to the calculated profiles of our samples. This behavior has a strong dependence on the content of water in the NBF and will be presented elsewhere. Our calculated total electrostatic potential is nearly constant at the core, with a negative value of about $-1.69 e/\text{\AA}$. Although not directly comparable, in Ref. [19] thicker NB films with up to 11.94 water molecules per amphiphilic were studied with an all-atom MD simulation and also a strong polarization of water was found at the interface with the head layers. Their measured electrostatic potential is also nearly constant at the core, but with a much smaller negative value of about $-0.2 \text{ Volt} = -0.0139 e/\text{\AA}$ for the sample of 11.94 water molecules per amphiphilic. Unfortunately there is not experimental data available for comparison, but nevertheless, in Ref. [45] the origin of the short-range and strong repulsive force between two ionic surfactant layers is calculated as decaying exponentially with their distance.

Fig. 5 (b) includes the contribution of macroscopic electric field E to our measured total forces on water, ions and chain molecules, as a function of the centers of mass location, averaged over a MD free trajectory of 100 ps. Units: $[F] = kJ/mol/\text{\AA}$. Due to the macroscopic electric field, the negatively charged amphiphilics tend to drift away of the

bilayer but this tendency is balanced by a contrary force on the mobile ions, that remain within the water layer. When adding all molecule - molecule interactions, the total forces (an order of magnitude lower than those due to the macroscopic field) on the amphiphilics tend to maintain a bilayer structure with the water inside.

VII. CONCLUSION:

In this paper we studied a simple model of a amphiphilic bilayer, a Newton black film, and analyzed the key *rôle* of the electrostatic interactions in their self-assembly. The model is simple enough so a large number of molecules can be included in the MD samples, but also detailed enough so as to take into account molecular charge distributions, flexible amphiphilic molecules and a reliable model of water. All these properties are essential to obtain a reliable conclusion.

The presented amphiphilic molecular model is extremely simple, but includes all main characteristics of these type of molecules: a strongly charged head atoms and a tail consisting in a semiflexible chain of hydrocarbon united atoms. As an example of its versatility we studied samples with a tail of 12 atoms and other of 18 atoms. This amphiphilic model also allows to study, in a simple way, the properties of bilayers formed by charged or neutral amphiphilics and with or without explicitly including water molecules in the numerical simulations.

As for the calculation of the electrostatic interactions, we also propose a novel and more accurate method to calculate the macroscopic electric field in cuasi 2D geometries, which can be easily included in any numerical calculation. The method, that essentially is a coarse grain fit of the macroscopic electric field beyond the dipole order approximation, was applied here to symmetrical bilayers (along the normal to the bilayer and with periodic boundary conditions in two dimensions), but their derivation is general and valid also for asymmetrical slab geometries.

Lastly, we emphasize the relevance and utility of these simple bilayer models. They can

be applied to the systematic study of the physical properties of these bilayers, that strongly depend not only on 'external parameters', like surface tension and temperature, but also on the kind of guest molecules embedded in them (eg. proteins, etc.). In turn, the structure and dynamics of the embedded molecules strongly depend on their interactions with the bilayer and with the surrounding water.

These simple bilayers can also be extremely useful to model, for example, the synthesis of inorganic (ordered or disordered) materials *via* an organic agent, which are based on the use of these self-assembling molecules [9]. This is a recent and very fast growing research field of nanotechnological relevance, as are lithography, etching and molding devices at the nanoscopic scale. Another fast developing field is that of electronic sensors and nanodevices supported on lipid bilayers [4, 46].

Furthermore, the amphiphilic bilayers are hosts for the diffusion and/or nucleation of guest molecules of relevance in biological and/or ambient problems, these studies are currently being performed.

Lastly, as our model retains the flexibility of the original amphiphilics, and the electrostatic interactions are included, the approach is really useful to obtain 'realistic' solutions to the above mentioned problems as well as those related to electric fields and electrostatic properties.

Acknowledgments

Z. G. greatly thanks careful reading and helpful suggestions to J. Hernando.

A: Correction terms for the atom-atom interactions within the slab and beyond the cut-off radius

In 3D samples, correction terms to the energy $U^{3D}(R_{cut})$ and virial $Vir^{3D}(R_{cut})$, due to the finite cut-off radius of the LJ site-site interactions, are calculated assuming a uniform distribution of sites beyond the cut-off radius R_{cut} . These terms are:

$$U^{3D}(R_{cut}) = \int_0^\pi \sin \theta d\theta \int_{R_{cut}}^\infty U_{LJ}(r) 2\pi r^2 dr = \frac{4\pi}{3} \varepsilon \sigma^3 \left[\frac{1}{3} \left(\frac{\sigma}{R_{cut}} \right)^9 - \left(\frac{\sigma}{R_{cut}} \right)^3 \right], \text{ and}$$

$$Vir^{3D}(R_{cut}) = \int_0^\pi \sin \theta d\theta \int_{R_{cut}}^\infty \left(-r \frac{\partial U_{LJ}(r)}{\partial r}\right) 2\pi r^2 dr = 8\pi\epsilon\sigma^3 \left[\frac{2}{3} \left(\frac{\sigma}{R_{cut}}\right)^9 - \left(\frac{\sigma}{R_{cut}}\right)^3 \right].$$

In our 2D samples, instead, the integrals are over the volume outside the R_{cut} radius and inside the slab. In all of our cases the width of the slab z_{slab} is larger than the diameter of the cut-off sphere ($z_{slab} > 2R_{cut}$), and the correction terms are then simply calculated.

$$U^{2D}(R_{cut}) = \int_0^\pi \sin \theta d\theta \int_{R_{cut}}^{R_{max}(\theta)} U_{LJ}(r) 2\pi r^2 dr,$$

where θ is the azimuthal angle measured from the perpendicular to the bilayer and $R_{max}(\theta) = \frac{z_{slab}}{2 \cos(\theta)}$.

The final result is:

$$U^{2D}(R_{cut}) = U^{3D}(R_{cut}) - \frac{4\pi}{3}\epsilon\sigma^3 \left[\frac{1}{30} \left(\frac{2\sigma}{z_{slab}}\right)^9 - \frac{1}{4} \left(\frac{2\sigma}{z_{slab}}\right)^3 \right].$$

In a similar way we obtain:

$$\begin{aligned} Vir^{2D}(R_{cut}) &= \int_0^\pi \sin \theta d\theta \int_{R_{cut}}^{R_{max}(\theta)} \left(-r \frac{\partial U_{LJ}(r)}{\partial r}\right) 2\pi r^2 dr \\ &= Vir^{3D}(R_{cut}) - 4\pi\epsilon\sigma^3 \left[\frac{4}{30} \left(\frac{2\sigma}{z_{slab}}\right)^9 - \frac{1}{2} \left(\frac{2\sigma}{z_{slab}}\right)^3 \right], \end{aligned}$$

and for the component along z (used to control the pressure along the perpendicular to the bilayer):

$$\begin{aligned} Vir_z^{2D}(R_{cut}) &= \int_0^\pi \sin \theta d\theta \int_{R_{cut}}^{R_{max}(\theta)} \left(-z \frac{\partial U_{LJ}(r)}{\partial z}\right) 2\pi r^2 dr \\ &= \frac{1}{3} Vir^{3D}(R_{cut}) - \frac{4\pi}{3}\epsilon\sigma^3 \left[\frac{1}{3} \left(\frac{2\sigma}{z_{slab}}\right)^9 - \left(\frac{2\sigma}{z_{slab}}\right)^3 \right]. \end{aligned}$$

On the other hand, if $z_{slab} < 2R_{cut}$, the calculated terms are:

$$\begin{aligned} U^{2D}(R_{cut}) &= U^{3D}(R_{cut}) \frac{z_{slab}}{2R_{cut}} - \frac{4\pi}{3}\epsilon\sigma^2 z_{slab} \left[\frac{1}{30} \left(\frac{\sigma}{R_{cut}}\right)^9 - \frac{1}{4} \left(\frac{\sigma}{R_{cut}}\right)^3 \right], \\ Vir^{2D}(R_{cut}) &= Vir^{3D}(R_{cut}) \frac{z_{slab}}{2R_{cut}} - 4\pi\epsilon \frac{z_{slab}}{R_{cut}} \sigma^3 \left[\frac{4}{30} \left(\frac{2\sigma}{z_{slab}}\right)^9 - \frac{1}{2} \left(\frac{2\sigma}{z_{slab}}\right)^3 \right], \text{ and} \\ Vir_z^{2D}(R_{cut}) &= \left(\frac{z_{slab}}{2R_{cut}}\right)^3 \left[\frac{1}{3} Vir^{3D}(R_{cut}) - U^{3D}(R_{cut}) \right]. \end{aligned}$$

B: The electrostatic macroscopic field model

We propose a superposition of slabs, upper and lower surfaces with opposite charges, but with a gaussian distribution, of width σ , along the depth of the slab. The charge distribution, electrostatic potential and electric field expressions are given in the following subsections, in order of increasing complexity. Case C.2 is the one we use for the reaction field in our MD simulations.

The results showed here correspond to a symmetrical distribution of charges, in the bilayer, about the origin (i. e. identical charges, widths and location of the maximums

along $\pm z$ axis. But for an asymmetrical case the calculation is straightforward, and the obtained result should be very useful for studying these bilayers under an applied external electric field, for example.

B1: The macroscopic electric field of a single slab:

First of all we review the well known case of an uniformly charged surface (ρ per unit area) located at $z = 0$. The potential field at z , due to this infinite, uniformly charged (xy) plane is:

$$V(z) = \int_0^\infty \rho \frac{2\pi r dr}{\sqrt{z^2+r^2}} = 2\pi\rho [\sqrt{x}]_{z^2}^\infty,$$

and the electric field is:

$$E(z) = -\frac{\partial V(z)}{\partial z} = 2\pi\rho \frac{z}{|z|}.$$

For a homogeneous dielectric single slab (of width $2z_i$), the macroscopic electric field is calculated assuming an uniformly charged plane at z_i (q_i per unit area) and another with opposite charge ($-q_i$ per unit area) located at $-z_i$. The potential field of this charge distribution is:

$$V(z) = 2\pi q_i ([\sqrt{x}]_{(z-z_i)^2}^\infty - [\sqrt{x}]_{(z+z_i)^2}^\infty) = -2\pi q_i (|z - z_i| - |z + z_i|), \text{ that is,}$$

$$V(z) = \begin{cases} -4\pi q_i z_i & \text{if } z < -z_i \\ 4\pi q_i z & \text{if } -z_i \leq z \leq z_i \\ 4\pi q_i z_i & \text{if } z_i > z \end{cases}.$$

The electric field of this charge distribution is:

$$E(z) = -4\pi q_i, \text{ if } -z_i \leq z \leq z_i, \text{ and } E(z) = 0 \text{ if } z < -z_i \text{ or } z > z_i.$$

Usually this result is given in terms of the the total dipole moment of the slab per unit area, which is $M_z = 2q_i z_i$, the macroscopic electric field then is $E_z = -\frac{2\pi}{z_i} M_z$, and the contribution of this charge distribution to the total energy of the system is $\frac{\pi}{z_i} M_z^2$.

If instead of considering two uniformly opposite charged planes, we consider that the charges show a certain spread along z , we can analyze a model of two gaussian charge distributions along z , of total charge $\pm q_i$ (per unit area) each one, standard deviation σ_i and maximum located at $\pm z_i$ respectively, and the charge distribution across the slab becomes

now:

$$\rho(z) = \frac{q_i}{\sqrt{2\pi}\sigma_i} \left(\exp\left(-\frac{(z-z_i)^2}{2\sigma_i^2}\right) - \exp\left(-\frac{(z+z_i)^2}{2\sigma_i^2}\right) \right) .$$

The total dipole moment of this system is again $M_z = 2q_i z_i$, but the potential $V(z)$ will differ. For the sake of simplicity we take as equal the dispersion of both distribution and we obtain:

$$V(z) = -2\pi \int_{-\infty}^{\infty} \rho(t) |z-t| dt = -2\pi \left(\int_{-\infty}^z \rho(t)(z-t) dt + \int_z^{\infty} \rho(t)(t-z) dt \right).$$

Replacing the $\rho(t)$ function we first obtain:

$$V(z) = -\sqrt{2\pi} \frac{q_i}{\sigma} \left(\int_{-\infty}^z \exp\left(-\frac{(t-z_i)^2}{2\sigma^2}\right) (z-t) dt - \int_{-\infty}^z \exp\left(-\frac{(t+z_i)^2}{2\sigma^2}\right) (z-t) dt + \int_z^{\infty} \exp\left(-\frac{(t-z_i)^2}{2\sigma^2}\right) (t-z) dt - \int_z^{\infty} \exp\left(-\frac{(t+z_i)^2}{2\sigma^2}\right) (t-z) dt \right),$$

and finally the potential is:

$$V(z) = -2\sqrt{2\pi}\sigma q_i \left(\exp\left(-\frac{(z-z_i)^2}{2\sigma^2}\right) - \exp\left(-\frac{(z+z_i)^2}{2\sigma^2}\right) \right) - (z-z_i) 2\pi q_i \left(\text{Erf}\left[\frac{(z-z_i)}{\sqrt{2}\sigma}\right] - \text{Erf}\left[\frac{(z+z_i)}{\sqrt{2}\sigma}\right] \right).$$

From this function, the electric field across a single slab, centered at $z = 0$, is:

$$E(z) = -\frac{\partial V(z)}{\partial z} = 2\pi q_i \left(\text{Erf}\left[\frac{(z-z_i)}{\sqrt{2}\sigma}\right] - \text{Erf}\left[\frac{(z+z_i)}{\sqrt{2}\sigma}\right] \right).$$

When $\sigma \rightarrow 0$, the functions tend to those found in electrostatics textbooks.

B2: Several neutral slabs model for the quasi-2D macroscopic electric field:

The typical charge distribution of our samples of amphiphilic bilayers can be decomposed in a linear superposition of neutral slabs. Replacing for each slab the uniformly charged faces by gaussian distributions of charges along z , of total charge $\pm q_i$ each one, width σ_i and located at $\pm z_i$, the preceding formulae in C.1 can be easily extended to any number of slabs and the final results are:

$$\begin{aligned} \rho(z) &= \sum_i \frac{q_i}{\sqrt{2\pi}\sigma_i} \exp\left(-\frac{(z-z_i)^2}{2\sigma_i^2}\right) , \\ V(z) &= -2\sqrt{2\pi} \sum_i \sigma_i q_i \left(\exp\left(-\frac{(z-z_i)^2}{2\sigma_i^2}\right) - \left(\frac{z-z_i}{\sqrt{2}\sigma_i}\right) \text{Erf}\left[\frac{(z-z_i)}{\sqrt{2}\sigma_i}\right] \right) . \\ E(z) &= -\frac{\partial V(z)}{\partial z} = 2\pi \sum_i q_i \text{Erf}\left[\frac{(z-z_i)}{\sqrt{2}\sigma_i}\right]. \end{aligned}$$

The accumulated energy of this superposition of slabs is:

$$W = \frac{1}{2} \int_{-\infty}^{\infty} \rho(z)V(z) dz = - \sum_i \sum_j q_i q_j \frac{\sigma_j}{\sigma_i} (I_1 + \sqrt{\pi} I_2).$$

The integral I_1 can be solved using the well known property of gaussians: the product of two gaussians is a third gaussian, in this case:

$$I_1 = \int_{-\infty}^{\infty} \exp\left(-\frac{(z-z_i)^2}{2\sigma_i^2}\right) \exp\left(-\frac{(z-z_j)^2}{2\sigma_j^2}\right) dz = \frac{\sqrt{\pi}}{\sqrt{\gamma}} \exp\left(-\frac{(z_i-z_j)^2}{2(\sigma_i^2+\sigma_j^2)}\right); \text{ with } \gamma = \frac{(\sigma_i^2+\sigma_j^2)}{\sigma_i^2\sigma_j^2}.$$

The second integral is a new mathematical solution and was solved with the aid of refs. [47, 48]. From the first one [47] we obtain:

$$I_{2a} = \int_{-\infty}^{\infty} \exp(-a(t-c)^2) \operatorname{erf}(t) dt = \sqrt{\frac{\pi}{a}} \operatorname{erf}\left(\frac{\sqrt{ac}}{\sqrt{1+a}}\right), \text{ and from the second reference:}$$

$$I_{2b} = \int_{-\infty}^{\infty} t \exp(-a(t-c)^2) \operatorname{erf}(t) dt = c I_{2a} + \frac{1}{a\sqrt{1+a}} \exp(-ac^2 + \frac{a^2 c^2}{1+a}). \text{ Finally, and taking}$$

$$a = (\sigma_j/\sigma_i)^2 \text{ and } c = \frac{(z_i-z_j)}{\sqrt{2}\sigma_j}, \text{ we calculate:}$$

$$I_2 = \int_{-\infty}^{\infty} \exp\left(-\frac{(z-z_i)^2}{2\sigma_i^2}\right) \left(\frac{z-z_j}{\sqrt{2}\sigma_j}\right) \operatorname{Erf}\left[\frac{(z-z_j)}{\sqrt{2}\sigma_j}\right] = \sqrt{2}\sigma_j I_{2b}.$$

This formulae is extremely simple to include, and fast to calculate in a MD or MC simulation. The application to other geometries is also straightforward. These relationships are also valid to apply when working with systems where there is a finite difference of voltage through the slab, keeping in mind that the total charge of the slab is zero.

-
- [1] D. Chandler, *Nature* **437**, 640 (2005).
 - [2] D. E. Discher, V. Ortiz, G. Srinivas, M. L. Klein, Y. Kim, D. Christian, S. Cai, P. Photos and F. Ahmed, *Prog. Polym. Sci.* **32**, 838 (2007).
 - [3] S. Vemparala, C. Domene and M. L. Klein, *Biophys. J.* **94**, 4260 (2008).
 - [4] X. Zhou, J. M. Moran Mirabal, H. G. Craighead and P. L. McEuen, *Nature Nanotech.* **2**, 185 (2007).
 - [5] E. Reimhult and K. Kumar, *Trends in Biotechnology* **26**, 82 (2008).
 - [6] J. J. Benattar, M. Nedyalkov, J. Prost, A. Tiss, R. Verger, C. Guilbert, *Phys. Rev. Lett.* **82**, 5297 (1999).
 - [7] V. Petkova, J. J. Benattar and M. Nedyalkov, *Biophys. J.* **82**, 541 (2002).
 - [8] X. L. Wu and A. Libchaber, *Phys. Rev. Lett.* **84**, 3017 (2000).
 - [9] K. J. Edler, *Phil. Trans. R. Soc. Lond. A* **362**, 2635 (2004).
 - [10] E. Mileva and D. Exerowa, *Adv. Colloid Interface Sci.* **100-102**, 547 (2003).
 - [11] C. Castellano, J. Generosi, A. Congiu and R. Cantelli, *Appl. Phys. Lett.* **89**, 233905 (2006).
 - [12] V. Castelleto, I. Cantat, D. Sarker, R. Bausch, D. Bonn, J. Meunier, *Phys. Rev. Lett.* **90**, 048302 (2003).
 - [13] D. S. Dean and R. R. Horgan, *Phys. Rev. E* **65**, 061603 (2002).

- [14] Z. Gamba, J. Hautman, J. Shelley and M. L. Klein, *Langmuir* **8**, 3155 (1992).
- [15] O. Belorgey and J. J. Benattar, *Phys. Rev. Lett.* **66**, 313 (1991).
- [16] F. Bresme and J. Faraudo, *Langmuir* **20**, 5127 (2004).
- [17] J. B. Klauda, B. R. Brooks and R. W. Pastor, *J. Chem. Phys.* **125**, 144710 (2006).
- [18] S. S. Jang and W. A. Goddard III, *J. Phys. Chem. B* **110**, 7992 (2006).
- [19] J. Faraudo and F. Bresne, *Phys. Rev. Lett.* **92**, 236102 (2004).
- [20] M. P. Allen and D. J. Tildesley, “Computer simulation of liquids”, Clarendon Press - Oxford (1990).
- [21] R. M. Levy and E. Gallicchio, *Ann. Rev. Phys. Chem.* **49**, 531 (1998).
- [22] A. Y. Toukmaji and J. A. Board Jr., *Comp. Phys. Communications* **95**, 73 (1996).
- [23] L. N. Kantorovich and I. I. Tupitsyn, *J. Phys.: Condens. Matter* **11**, 6159 (1999).
- [24] J. A. Hernando, *Phys. Rev. A* **44**, 1228 (1991).
- [25] S. W. de Leeuw and J. W. Perram, *Mol. Phys.* **37**, 1313 (1979).
- [26] A. Brodka and A. Grzybowski, *J. Chem. Phys.* **117**, 8208 (2002).
- [27] I. Yeh and M. L. Berkowitz, *J. Chem. Phys.* **111**, 3155 (1999).
- [28] P. Padilla and S. Toxvaerd, *J. Chem. Phys.* **94**, 5850 (1991).
- [29] J. Shelley, K. Watanabe and M. L. Klein, *Int. Quantum Chem: Quantum Biol. Symp.* **17**, 103 (1990).
- [30] M. W. Mahoney and W. L. Jorgensen, *J. Chem. Phys.* **112**, 8910 (2001).
- [31] M. W. Mahoney and W. L. Jorgensen, *J. Chem. Phys.* **114**, 363 (2001).
- [32] Ciccotti G., M. Ferrario and Ryckaert J. P., *Mol. Phys.* **47**, 1253 (1982).
- [33] Z. Gamba and B. M. Powell, *J. Chem. Phys.* **112**, 3787 (2000).
- [34] C. Pastorino and Z. Gamba, *J. Chem. Phys.* **115**, 9421 (2001).
- [35] C. Pastorino and Z. Gamba, *J. Chem. Phys.* **119**, 2147 (2003).
- [36] M. Krack, A. Gambirasio and M. Parrinello, *J. Chem. Phys.* **117**, 9409 (2002).
- [37] H. Nada, J. P. J. M. van der Eerden, *J. Chem. Phys.* **118**, 7401 (2003).
- [38] D. Andelman, *Handbook of Biological Physics*, Vol. 1, chapter 12, eds. R. Lipowsky and E. Sackman (1995).
- [39] J. F. Nagle and S. Tristram-Nagle, *Biochim. Biophys. Acta* **1469**, 159 (2000).
- [40] N. Kucerka, J. F. Nagle, S. E. Feller and P. Balgavý, *Phys. Rev. E* **69**, 51903 (2004).
- [41] G. Martyna, M. L. Klein and M. Tuckerman, *J. Chem. Phys.* **97**, 2635 (1992).

- [42] H. J. C. Berendsen, J. P. M. Postma, A. DiNola and J. R. Haak, *J. Chem. Phys.* **81**, 3684 (1984).
- [43] G. Ropars, D. Chauvat, A Le Floch, M. N. O'Sullivan-Hale and R. W. Boyd, *Appl. Phys. Lett.* **88**, 234104 (2006).
- [44] D. C. Clark, R. Dann, A. R. Mackie, J. Mingins, A. C. Pinder, P. W. Purdy, E. J. Russell, L. J. Smith and D. R. Wilson, *J. Colloid Interface Sci.* **138**, 195 (1990).
- [45] J. Faraudo and F. Bresme, *Phys. Rev. Lett.* **94**, 077802 (2005).
- [46] E. T. Castellana, P. S. Cremer, *Surface Science Reports* 61, 429 (2006).
- [47] G. Thomas, http://www.csc.fi/math_topics/Mail/NANET94/msg00289.html, (1994).
- [48] Web site: <http://www.integrals.com>, open site of Wolfram Research, Inc.